Nonstationary effects in velocity-selective optical pumping

Wojciech Gawlik
Instytut Fizyki, Uniwersytet Jagielloński, 30-059 Kraków, ul. Reymonta 4, Poland
(Received 29 May 1986)

Time-dependent analysis of nonstationary effects in velocity-selective optical pumping is performed with a four-level model for weak light intensities. No phenomenological relaxation constants are introduced and the nonstationary effects are obtained as the consequence of averaging the time evolution of individual atoms in a vapor phase moving in the light fields when typical pumping times are comparable with the finite laser-beam transit times. Under appropriate conditions strong deformation of the population distribution of the long-lived lower state occurs, which in the case of polarization spectroscopy is responsible for the appearance of a dip (possibly narrower than the homogeneous linewidth) in the center of a Doppler-free resonance. The theoretical results are in a good qualitative agreement with the recent experimental observations.

I. INTRODUCTION

Velocity-selective optical pumping (VSOP), i.e., a redistribution of populations of lower-state sublevels of atoms belonging to a given velocity class, has been found to be a very important mechanism in Doppler-free laser spectroscopy.[1–8] The standard approach to VSOP is based on steady-state density matrix or rate equations where the relaxation and possible finite laser-beam transit-time effects are accounted for with the help of phenomenological rates. Although such an approach proved to be very useful in many applications, some experimental observations have been recently performed[9–14] which cannot be explained with the steady-state theories.

Bjorkholm *et al.*[10] have described strong deformations of two-photon line shapes attributed to nonstationary effects in VSOP and conclude that the standard theory with phenomenological rates is inadequate for their description. It turns out that similar nonstationary effects are responsible also for narrow dips observed by Gawlik *et al.*[11,12] with the help of polarization spectroscopy (PS). Recently, Thomas and Forber[13] have reported on nonexponential decay of a photon-echo amplitude which also could not be explained with a simple transit rate, and Klimcak and Camparo[14] have described optical-pumping dips in a homogeneously broadened line.

Effects of finite transit time in saturated absorption spectroscopy (SAS) of two-level systems without optical pumping have been discussed in Ref. 15, in two-photon spectroscopy in Ref. 16, and, more recently, by Thomas and Quivers[9] in optical pumped three-level systems.

While the transit-time effects analyzed in Refs. 9, 15, and 16 are responsible for rather subtle modifications of the line shapes, the effects described by Bjorkholm *et al.*,[10] Gawlik *et al.*,[11,12] and Klimcak and Camparo[14] are by no means small. On the contrary, they provide a rather spectacular illustration of the importance of the nonstationary effects.

The optical-pumping dips of Refs. 10 and 14 and the dips described by Gawlik *et al.* are similar in that they both result from the nonstationarity of optical pumping. However, they reflect this nonstationary situation in various ways. In the case of polarization spectroscopy (Refs. 11 and 12) the probe beam is required to do some optical pumping, while the dips of Refs. 10 and 14 occur even with negligible light intensity. Moreover, the homogeneous optical pumping dips of Ref. 14 are only observed for atoms probed after the process of optical pumping has been completed, whereas the dips of Refs. 10–12 are observed during the process of optical pumping. This distinction manifests the fact that there are various ways in which optical pumping can affect a spectral line shape.

In this paper we give a theoretical analysis of such nonstationary effects with the help of a simple four-level model where the lower state possesses an appropriate structure allowing for optical pumping. For the sake of comparison with the experimental work[11,12] we will refer mainly to the results obtained in PS, but the main conclusions apply also to other spectroscopic techniques where optical pumping (not necessarily velocity selective) can take place. In Sec. II the experimental situation, fields, and atomic system are specified. In Sec. III we introduce time-dependent rate equations (derived in the Appendix) and solve them under given conditions. In Sec. IV, which is the main part of the paper, we express the probe-beam signals in PS in terms of atomic populations, discuss time evolution of the populations and the transit-time effects under nonstationary conditions of VSOP, calculate theoretical PS signals which exhibit narrow dips, and finally, we briefly discuss many-line interference effects.

II. MODEL OF ATOMIC SYSTEM AND EXPERIMENTAL SITUATION

A. Experimental situation

Our analysis concerns the experimental situation where investigated atoms in an absorption cell are irradiated with two counterpropagating beams, the pump and the probe originating from the same laser. The pumping beam is circularly polarized (e.g., σ^+), whereas the probe

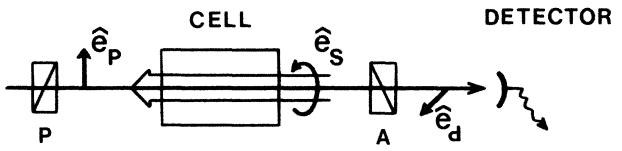

FIG. 1. Schematical setup for studying VSOP with two counterpropagating beams: the probing beam linearly polarized ($\hat{\mathbf{e}}_p=\hat{\mathbf{e}}_x$), and the pumping beam polarized differently than $\hat{\mathbf{e}}_p$ (e.g., circularly, $\hat{\mathbf{e}}_s=\hat{\mathbf{e}}_+$). If analyzer A and polarizer P are orthogonal ($\hat{\mathbf{e}}_p\cdot\hat{\mathbf{e}}_d\approx 0$) the setup allows studies of PS; if P and A are parallel ($\hat{\mathbf{e}}_p\cdot\hat{\mathbf{e}}_d=1$) SAS can be studied.

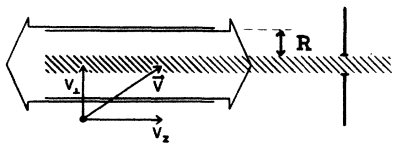

FIG. 2. Geometry of the light beams and an additional aperture selecting very narrow axial part of the probe beam for detection. R denotes the difference between equal radii of the beams and that of the shaded detection region. $v_\perp$ and v_z are transversal and longitudinal, respectively, components of the velocity $\mathbf{v}$ of an atom moving across the beams.

is linearly polarized. We record the intensity of that component of the probe beam which passes a linear analyzer placed between the cell and detector (Fig. 1). Depending on an angle between the direction of the incident probe-beam polarization $\hat{\mathbf{e}}_p$ and the analyzer's axis $\hat{\mathbf{e}}_d$ we can realize either the case of polarization spectroscopy or of saturated absorption spectroscopy: For analyzer A crossed (or nearly crossed) with polarizer P ($\hat{\mathbf{e}}_p\cdot\hat{\mathbf{e}}_d\approx 0$) we have the situation typical for PS. On the other hand, if the analyzer is parallel with the polarizer ($\hat{\mathbf{e}}_p\cdot\hat{\mathbf{e}}_d=1$) we have the case of SAS.

For the sake of simplicity we consider here only the case when the pump beam is circularly polarized. It is quite straightforward, however, to discuss also other situations characteristic for PS or SAS within our simple model. For instance, if an appropriate transformation of a reference frame from the $\{|0\rangle,|\pm1\rangle\}$ circular basis to the $\{|x\rangle,|y\rangle,|z\rangle\}$ one is performed, the case when the pumping beam is linearly polarized at 45° to $\hat{\mathbf{e}}_p$ can be readily discussed[17] with the help of the energy-level diagram of Fig. 3 and the rate equations from Sec. III below.

In the following we shall concentrate exclusively on PS. It should be remembered, however, that many results of this paper are more general.

To make the analysis as simple as possible we assume that both light beams are overlapping and have the same diameters and uniform intensity distributions. It is not very difficult to fulfill this condition in practice by using appropriate diaphragms for selection of the central region of the Gaussian laser beams, but, if necessary, the quantities $I_\pm, I_s$ in Eqs. (4) and (5) below could also be considered as space dependent. One could study either a general space dependence of $I_\pm, I_s$, or a simpler case when the beams have uniform intensity distributions but different diameters. The time evolution of the populations of an individual atom in the latter case consists of periods within which the atom interacts either with a single beam or with two beams, and can be easily calculated for each of those periods along the lines of this paper. Possible x-y dependence of the light fields does not change the main qualitative results of this analysis so we will ignore it.

Figure 2 shows the assumed geometry of the light beams and an additional aperture selecting the very narrow axial part of the probe beam for detection. The difference between the light beams and the shaded detection region radii is denoted by R.

B. Fields

The net electric field of both light beams counterpropagating along the $0z$ direction is

$$\mathbf{E}(z,t)=\mathscr{E}\cos(\omega t-kz)+\mathscr{E}'\cos(\omega t+kz)\ , \tag{1a}$$

where $\mathscr{E},\mathscr{E}'$ are the amplitudes of the pumping and probing beams respectively and k is the magnitude of the wave vector. The pump beam is σ^+ polarized and the probe beam is polarized linearly along the $0x$ axis, so that we have

$$\mathbf{E}(z,t)=\frac{\mathscr{E}}{2}\hat{\mathbf{e}}_+e^{-i(\omega t-kz)}+\frac{\mathscr{E}'}{2}\hat{\mathbf{e}}_xe^{-i(\omega t+kz)}+\text{c.c.}\ , \tag{1b}$$

where $\hat{\mathbf{e}}_\pm=\mp(1/\sqrt{2})(\hat{\mathbf{e}}_x\pm i\hat{\mathbf{e}}_y)$.

With the field given by Eq. (1) we can write matrix elements of the interaction Hamiltonian $V=-\mathbf{E}\cdot\mathbf{D}$,

$$\begin{aligned}V_{0+}&=-\beta'_+e^{-i(\omega t+kz)}+\text{c.c.}\ ,\\ V_{0-}&=-\beta e^{-i(\omega t-kz)}+\beta'_-e^{-i(\omega t+kz)}+\text{c.c.}\ ,\end{aligned} \tag{2}$$

where

$$\beta=\frac{\mathscr{E}d_-}{2\hbar}\ ,\quad \beta'_\pm=\frac{\mathscr{E}'d_\pm}{2\sqrt{2}\hbar} \tag{3}$$

are the Rabi frequencies for the pump and probe, respectively. Unless otherwise stated, different values of matrix elements $d_\pm=\langle 0|\hat{\mathbf{e}}_\mp\cdot\mathbf{D}|\pm\rangle$ are allowed for, hence the Rabi frequencies β'_+ and β'_- might also differ.

C. Atoms

The simplest possible model of atomic system that allows discussion of the nonstationary effects of velocity-selective optical pumping with polarized laser beams is a four-level system composed of a single $|J=0;m=0\rangle$ level as the upper state, and three degenerate Zeeman sublevels $|J=1;m=0,\pm1\rangle$ as the lower levels. In Fig. 3 we denote sublevels $m=-1,0,+1$ of the $J=1$ state as $|-\rangle$, $|1\rangle$, and $|+\rangle$, respectively, and mark transitions induced by the σ^+ polarized pump beam with double arrow and with single arrows those due to the probe. The frequency ω of the light waves is close to the frequency ω_0 of the transition $|J=0\rangle$-$|J=1\rangle$.

The upper state $|0\rangle$ can decay spontaneously to all lower sublevels. It is assumed that the collisional relaxa-

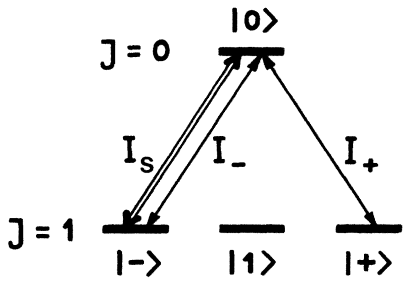

FIG. 3. Four-level system allowing discussion of the nonstationary effects of VSOP. The states $|-\rangle$, $|1\rangle$, and $|+\rangle$ are sublevels $m=-1,0,+1$, respectively, of the $J=1$ lower level, $|1\rangle$ playing the role of the trap level. $I_s, I_\pm$ are the pumping rates for the pump and the probe, respectively. Circularly polarized pump beam induces transitions marked with a double arrow, while the transitions induced by the linearly polarized probe beam are depicted with a single one.

tion of the lower levels is so slow that it can be neglected with respect to transit effects and the perturbation by light.

Level $|1\rangle$ is not directly perturbed by the light beams so it acts as the "trap level" in a way that atoms which have decayed to $|1\rangle$ cannot be further excited. The existence of such a trap level is essential for nonstationary effects discussed below. It should be noted that its role may be played by any stable level that can be populated by spontaneous emission from the upper state but cannot be further excited by the light beams. In particular, it could be an off-resonance hyperfine component of the lower level as in the case of alkali metals.[10,14] In our simple analysis, however, it is quite sufficient to consider the Zeeman sublevel $|J=1;m=0\rangle$ as the trap since it has all necessary properties, i.e., it is not directly perturbed by light of the given polarization.

To make our model more general we will calculate time evolution of the populations with the assumption that the branching ratios p_i from the upper state to sublevels $|i\rangle$ and the corresponding dipole matrix elements can be arbitrary (with $p_+ + p_- + p_1 = 1$). Changing p_1 would allow us then to control the effect of trapping on the dynamics of optical pumping, while different values of p_+ and p_- could be helpful for discussion of systems more complex than that of Fig. 3. Referring to the specific conditions of PS we will later take $p_+ = p_-$.

Despite its simplicity (particularly the assumption that only the lower state has some structure) the model gives very satisfactory results. This is due to the fact that for weak light intensities it is the optical pumping in the long-lived lower state which determines the characteristics of the observed signals.

III. RATE EQUATIONS

A full description of an atomic system interacting with a light field is provided by the generalized Bloch equations for the density matrix of the system. If, however, the intensity of the light beam is sufficiently weak, so that the coherence and strong-field effects can be neglected, a much simpler system of rate equations can satisfactorily describe the atom dynamics.

In the analysis presented in this paper we use the following system of rate equations for the populations of levels $|0\rangle$, $|+\rangle$, $|-\rangle$, and $|1\rangle$, (see Fig. 3), which have been derived in the Appendix:

$$\dot{n}_0 = (n_- - n_0)(I_s + I_-) + (n_+ - n_0)I_+ - \Gamma n_0 , \tag{4a}$$

$$\dot{n}_+ = -(n_+ - n_0)I_+ + p_+ \Gamma n_0 , \tag{4b}$$

$$\dot{n}_- = -(n_- - n_0)(I_s + I_-) + p_- \Gamma n_0 , \tag{4c}$$

$$\dot{n}_1 = p_1 \Gamma n_0 , \tag{4d}$$

where

$$I_s(\delta, kv_z) = 4(\beta^2/\Gamma)\mathcal{L}(\delta - kv_z) ,$$
$$I_\pm(\delta, kv_z) = 4(\beta_\pm'^2/\Gamma)\mathcal{L}(\delta + kv_z) \tag{5}$$

are frequency-, velocity-, and intensity-dependent pumping rates for the pump (I_s) and probe ($I_\pm$) beams; $\mathcal{L}(x) = 1/(1+4x^2/\Gamma^2)$; $\delta = \omega - \omega_0$; v_z is a longitudinal component of atomic velocity; Γ is the spontaneous decay rate of the upper state; and p_+, p_-, and p_1 are branching ratios of the decay from $|0\rangle$ into the $|+\rangle$, $|-\rangle$, and $|1\rangle$ states, respectively.

In spite of an essential role of level $|1\rangle$ as the trap for the fraction p_1 of the excited population n_0, Eq. (4d) brings no additional mathematical complication to the system of the first three equations (4a)–(4c), because the "trapped population" n_1 does not directly influence the remaining ones. This simplification results from negligence of nonradiative relaxation which could bring some possible mixing of the populations. Under such conditions the only important consequence of the trap level is the fact that $p_+ + p_- < 1$. It is not very difficult to include in Eqs. (4) relaxation other than spontaneous emission (e.g., collisions). However, as long as the spontaneous emission and the transit effects described below are the dominant processes, Eqs. (4) are quite adequate for discussion of the salient features of the considered phenomena.

As in Ref. 10 we do not introduce any phenomenological relaxation constants to account for finite transit times. Instead, we find the time-dependent solutions of Eqs. (4) and analyze their properties in the transient regime where optical pumping is nonstationary. The nonstationarity arises from the movement of atoms across spatially confined light beams which results in finite interaction times often being shorter than the time necessary for reaching steady-state conditions. In standard stationary approaches transit effects are accounted for by using steady-state solutions of the rate (or density matrix) equations with appropriate phenomenological relaxation constants. Such steady-state solutions, however, describe the effects of infinitely long interactions with the light beams when an equilibrium between pumping and relaxation had already been established. This approach with simple transit constants is inadequate (though widely used) when transit times across the light beams are finite and comparable with the pumping times determined as $(I_s, I_\pm)^{-1}$. In such cases time-dependent analysis of transit effects has

to be performed, or space-dependent relaxation rates should be used as suggested in Ref. 14.

We solve the system of Eqs. (4a)–(4c) with the initial condition at the time $t=0$ when a given atom enters the beams,

$$n_+(t=0)=n_-(t=0)=\mathcal{N}_0(v_z)\ , \tag{6}$$

$\mathcal{N}_0(v_z)$ being the initial equilibrium population of the lower-state sublevels (same for all sublevels).

The time-dependent normalized solutions are given by

$$\begin{bmatrix} n_0 \\ n_+ \\ n_- \end{bmatrix} = \sum_{i=1}^{3} C_i \begin{bmatrix} 1 \\ \dfrac{p_+\Gamma+I_+}{I_i} \\ \dfrac{p_-\Gamma+I_s+I_-}{J_i} \end{bmatrix} e^{\lambda_i t}\ , \tag{7}$$

where in the weak-field approximation ($I_s, I_\pm \ll \Gamma$) the coefficients C_i and eigenvalues of the characteristic equation are

$$\begin{aligned} C_1&=-C_0 2\alpha T(p_+J_2J_3-p_-I_2I_3)\ ,\\ C_2&=-C_0 I_2J_2(p_+J_3-p_-I_3)\ ,\\ C_3&=C_0 I_3J_3(p_+J_2-p_-I_2)\ ,\\ \lambda_1&=-\Gamma\ ,\\ \lambda_2&=-T(1+\alpha)\ ,\\ \lambda_3&=-T(1-\alpha)\ , \end{aligned}$$

with

$$\begin{aligned} C_0&=\mathcal{N}_0[2p_+p_-(I_s+I_--I_+)\Gamma\alpha T]^{-1}\ ,\\ I_i&=I_++\lambda_i,\ \ J_i=I_s+I_-+\lambda_i\ ,\\ \alpha&=[1-p_1I_+(I_s+I_-)T^{-2}]^{1/2}\ ,\\ T&=\tfrac{1}{2}[I_+(1-p_+)+(I_s+I_-)(1-p_-)]\ . \end{aligned} \tag{8}$$

If the decay rates into the $|+\rangle$ and $|-\rangle$ states are equal, $p_+=p_-=p=\frac{1}{2}(1-p_1)$, then $I_+=I_-=I_p$, and we can write C_i in a more compact form,

$$\begin{aligned} C_1&=-\mathcal{N}_0\frac{2I_p+I_s}{\Gamma}\ ,\\ C_2&=-\frac{\mathcal{N}_0}{2p}\frac{I_2J_2}{\Gamma\alpha T}\ ,\\ C_3&=\frac{\mathcal{N}_0}{2p}\frac{I_3J_3}{\Gamma\alpha T}\ , \end{aligned}$$

with

$$T=\tfrac{1}{4}(1+p_1)(2I_p+I_s)\ ,$$

and

$$\alpha=[1-p_1I_p(I_p+I_s)T^{-2}]^{1/2}\ .$$

Under the above conditions, i.e., with a weak-field approximation ($I_p, I_s \ll \Gamma$), $p_+=p_-$, and with the initial condition (6), solutions (7) can be written as

$$\begin{aligned} n_0(t)&=-\mathcal{N}_0\frac{2I_p+I_s}{\Gamma}e^{-\Gamma t}\\ &\quad-\frac{\mathcal{N}_0}{2p}\frac{I_2J_2}{\Gamma\alpha T}e^{-T(1+\alpha)t}+\frac{\mathcal{N}_0}{2p}\frac{I_3J_3}{\Gamma\alpha T}e^{-T(1-\alpha)t}\ ,\\ n_+(t)&=p\mathcal{N}_0\frac{2I_p+I_s}{\Gamma}e^{-\Gamma t}\\ &\quad+\frac{\mathcal{N}_0}{2}e^{-Tt}\left[\frac{I_s+I_p-T}{\alpha T}(e^{\alpha Tt}-e^{-\alpha Tt})\right.\\ &\quad\left.+e^{-\alpha Tt}+e^{\alpha Tt}\right]\ ,\\ n_-(t)&=p\mathcal{N}_0\frac{2I_p+I_s}{\Gamma}e^{-\Gamma t}\\ &\quad+\frac{\mathcal{N}_0}{2}e^{-Tt}\left[\frac{I_p-T}{\alpha T}(e^{\alpha Tt}-e^{-\alpha Tt})\right.\\ &\quad\left.+e^{-\alpha Tt}+e^{\alpha Tt}\right]\ . \end{aligned} \tag{9}$$

The first terms of Eqs. (9) represent a fast-transient behavior of the atomic populations after the atom has entered the interaction region at $t=0$, and are of the order of $(I_p,I_s)\Gamma^{-1}\exp(-\Gamma t)$. When the light intensities are weak and $t\gg\Gamma^{-1}$ those terms can be neglected.

Time evolution of the populations depends very strongly on the parameter α defined by Eq. (8). For a negligibly weak probe beam ($I_p \ll I_s$) and/or for absence of a trap level, i.e., $p_1=0$, $\alpha=1$ and in each of the above populations a stationary term different from zero appears. If the probe beam is not weak in comparison with I_s, $0<\alpha<1$ and all terms of Eqs. (9) decay to zero. It is therefore natural that the nonstationary effects of optical pumping show up only if the probe beam is appropriately strong and if the level structure under consideration includes a suitable trap level ($p_1\neq 0$).

IV. VELOCITY-SELECTIVE OPTICAL PUMPING

As discussed previously (Refs. 1–3), if the long-lived lower state is not single and the light intensities are not too strong, VSOP rather than saturation of an optical transition is responsible for the Doppler-free signals in polarization, as well as in saturated absorption spectroscopy.

Equations (9) allow, in principle, discussion of various specific effects, e.g., SAS with optical pumping, or probe-beam-induced fluorescence described in Ref. 14. For the sake of brevity, however, we shall limit the calculations only to the PS signals. In Sec. IV A we express the probe-beam signal in terms of atomic populations, in Sec. IV B we discuss the time evolution of the populations, and in Sec. IV C we analyze the transit-time effects.

A. Probe-beam signals in polarization spectroscopy

Macroscopic polarization $\mathcal{P}=\mathrm{Tr}(\mathbf{D}\rho)$ induced by the field (1) in the ensemble of atoms described in Sec. II C (Fig. 3) is

$$\mathscr{P}=\mathbf{D}_{-0}\rho_{0-}+\mathbf{D}_{+0}\rho_{0+}+\mathbf{D}_{0-}\rho_{-0}+\mathbf{D}_{0+}\rho_{+0}\ .$$

Making use of relation (A2) from the Appendix, $\mathscr{P}$ can be decomposed into the contributions due to the pumping and probing beams

$$\mathscr{P}=\mathbf{P}e^{-i(\omega t-kz)}+\mathbf{P}'e^{-i(\omega t+kz)}\ . \tag{10}$$

The probe-beam signals are determined by the second contribution in Eq. (10),

$$I_{\text{probe}}\sim\left|\left\langle\frac{\partial\mathbf{P}'}{\partial t}\cdot\hat{\mathbf{e}}_d\right\rangle\right|^2\ ,$$

where $\langle\ \rangle$ denotes ensemble averaging (for the situation considered the most important being the velocity averaging). Being concentrated on PS ($\hat{\mathbf{e}}_p\cdot\hat{\mathbf{e}}_d\approx 0$) we are mainly interested in the birefringence and dichroism of the investigated medium, which results in a difference between P'_+ and P'_-, i.e., the left and right circularly polarized components of P',

$$I_{\text{PS}}\sim|\langle P'_+-P'_-\rangle|^2\ . \tag{11}$$

(For the realization of PS with a linearly polarized pump at 45° to $\hat{\mathbf{e}}_p$, which we shall not discuss in detail, the probe-beam signal arises from a linear birefringence and dichroism, i.e., a difference between P'_x and P'_y.)

If $p_+=p_-$, according to Eqs. (A2) and (A5) from the Appendix, the components $P'_\pm$ are

$$P'_\pm=\frac{d\beta'}{\Omega_+}(n_0-n_\pm)\ ,$$

with $\Omega_+=\delta+kv_z-i\Gamma/2$, which for an excitation sufficiently weak to neglect n_0 ($n_0\ll n_\pm$) yields

$$P'_+-P'_-=-\frac{d\beta'}{\Omega_+}(n_+-n_-)\ .$$

Thus we arrive at the following expression for the probe-beam signal in PS:

$$I_{\text{PS}}\sim(d\beta')^2\left|\left\langle\frac{n_+-n_-}{\Omega_+}\right\rangle_v\right|^2\ . \tag{12}$$

Equation (12) explains the importance of velocity-selective optical pumping for Doppler-free polarization spectroscopy because the asymmetry of populations $\Delta n=n_+-n_-$ of the lower state, i.e., the lower-state polarization, is due to optical pumping by both beams.

B. Time evolution of Δn

According to Eq. (12) calculation of the probe-beam signals requires velocity averaging which consists of independent integration over transversal and longitudinal components of the velocity. Since the transversal components $v_\perp$ determine atomic transit times across laser beams of finite diameters, integration over $v_\perp$ is equivalent to integration over various times of interaction of individual atoms with the light. It is therefore important to perform a thorough discussion of the time dependence of the difference of the populations $\Delta n(t)$. Taking $t\gg\Gamma^{-1}$ we get easily from Eqs. (9)

$$\Delta n(t)=n_+-n_-=\frac{\mathcal{N}_0 I_s}{2\alpha T}(e^{-T(1-\alpha)t}-e^{-T(1+\alpha)t})\ . \tag{13}$$

Figure 4 shows the time dependence of Δn for atoms with zero longitudinal velocity $v_z=0$ in the case of a negligibly weak probe beam ($\beta'=2\times10^{-4}\Gamma$) when $\alpha=1$. The $\Delta n(t)$ dependence on the pump-beam intensity (expressed in terms of the Rabi frequency β) is presented in Fig. 4(a), and on the laser detuning from the exact resonance in Fig. 4(b). The effect of detuning is equivalent to decreasing the intensity of the pump, both leading to a decrease of the pump rate of atoms with $v_z=0$. Since for $\alpha=1$ one of the terms in Eqs. (9) and (13) becomes stationary, Δn monotonically increases with time until a stable maximum value of atomic polarization is reached. As the transit effects are the only relaxation processes which are taken into account in this analysis, the final maximum value of the lower-state polarization $\Delta n(t\to\infty)$ is $2\mathcal{N}_0/(1+p_1)$, i.e., $\frac{3}{2}\mathcal{N}_0$ for $p_1=\frac{1}{3}$, and even $2\mathcal{N}_0$ if there is no trapping ($p_1=0$).

Figure 5 shows the time dependence of Δn under the same conditions as before, except for the probe-beam in-

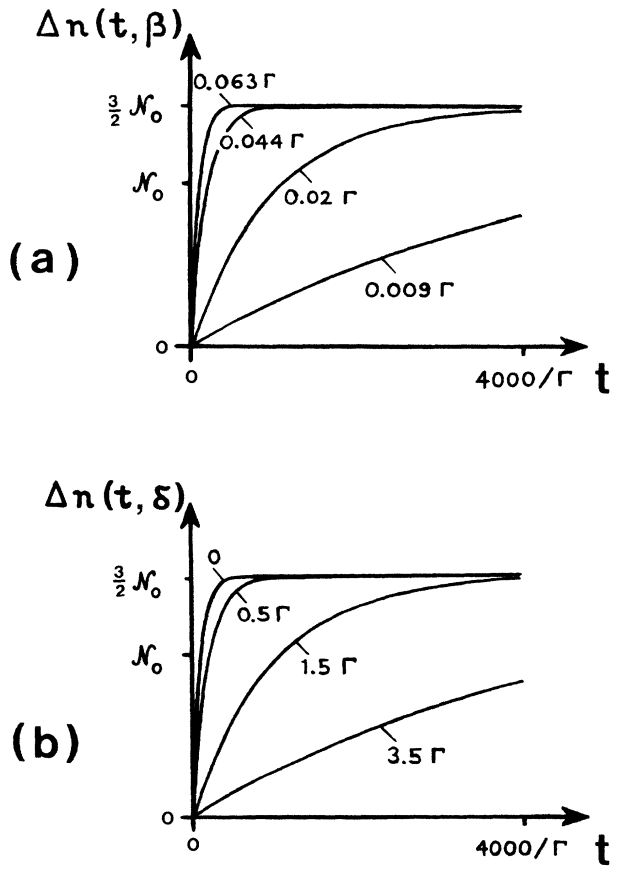

FIG. 4. $\Delta n(t)$ dependences for atoms with $v_z=0$ and a negligibly weak probe beam ($\beta'=2\times10^{-4}\Gamma$), i.e., when $\alpha=1$ (a) for $\delta=0$ and various intensities of the pump beam expressed in terms of the Rabi frequency β, (b) for $\beta=6.3\times10^{-2}\Gamma$ and various detunings δ.

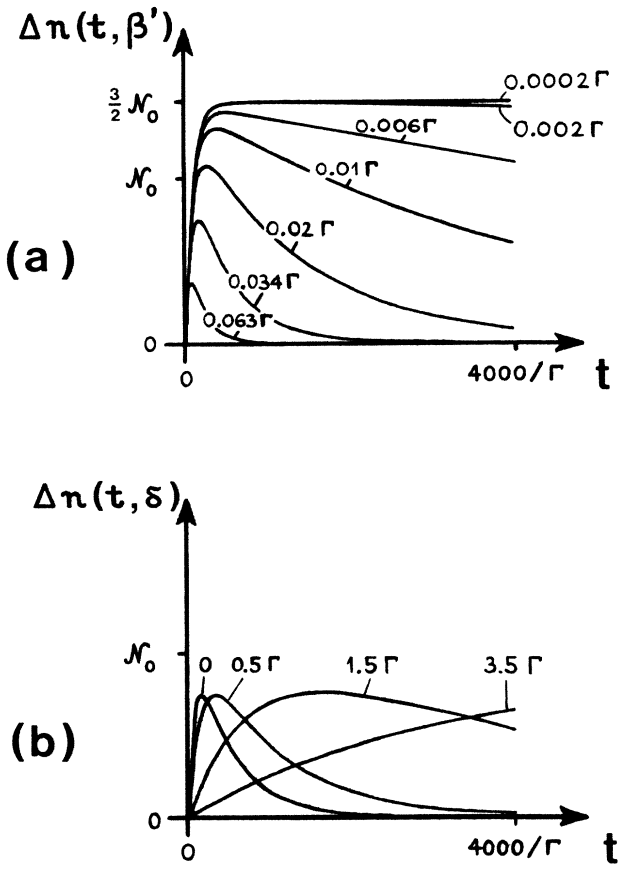

FIG. 5. $\Delta n(t)$ dependences for $v_z=0$, $\beta=6.3\times10^{-2}\Gamma$ and for a strong probe beam when $\alpha\leq1$ (a) for $\delta=0$ and various intensities of the probe beam (expressed in terms of β'), (b) for $\beta'=3.4\times10^{-2}\Gamma$ and various detunings δ.

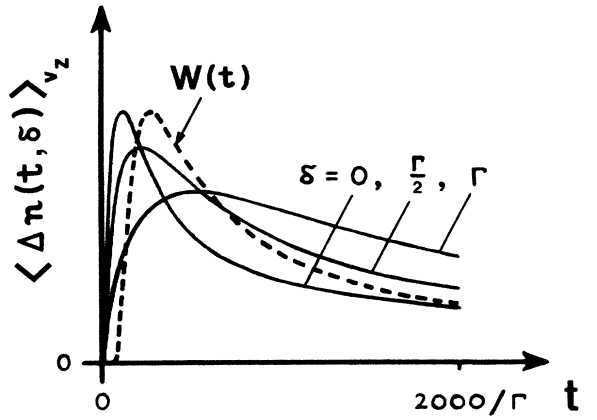

FIG. 6. Time dependence of Δn averaged over Doppler shifts for a strong probe beam ($\beta=3.4\times10^{-2}\Gamma$, $\beta'=7.7\times10^{-2}\Gamma$) and for various detunings δ. With a broken line the transit-line distribution $W(t)$ [Eq. (16)] is shown for typical experimental conditions with $R=1.5$ mm, $u=500$ m/s, and $\Gamma=1/\tau=6\times10^7$ s^{-1}.

tensity which is not negligible now, i.e., β' may be comparable with β which makes $\alpha<1$. Figure 5(a) shows the effect of the probe-beam intensity for zero detuning. It is seen that the strong probe beam is responsible for nonstationarity of the polarization Δn and for the reduction of its amplitude with respect to the case with $\alpha=1$ (Fig. 4). This is due to a depletion of both $|-\rangle$ and $|+\rangle$ states by pumping to the trap level $|1\rangle$ with the probe beam. Thus, if the two beams are strong, there is a competition between the probe which depletes both populations $n_\pm$ and the pump which builds up Δn. In Fig. 5(b) $\Delta n(t)$ is plotted for a strong probe and various laser detunings. Here it is seen that detuning from $\delta=0$ simply lengthens the time scale of the evolution. An important consequence of this fact is that after a given evolution time the off-resonance polarization $\Delta n(\omega\neq\omega_0)$ can be larger than the on-resonance one $\Delta n(\omega=\omega_0)$. It is important that this property holds also for Δn averaged over all longitudinal velocities, i.e., various Doppler shifts of the apparent frequencies of the two beams with respect to ω_0. Figure 6 shows $\langle\Delta n(t)\rangle_{v_z}$ for various δ and for $\beta=3.4\times10^{-2}\Gamma$, and $\beta'=7.7\times10^{-2}\Gamma$.

Under the experimental conditions with which we are concerned (see Fig. 2) the evolution time is determined by

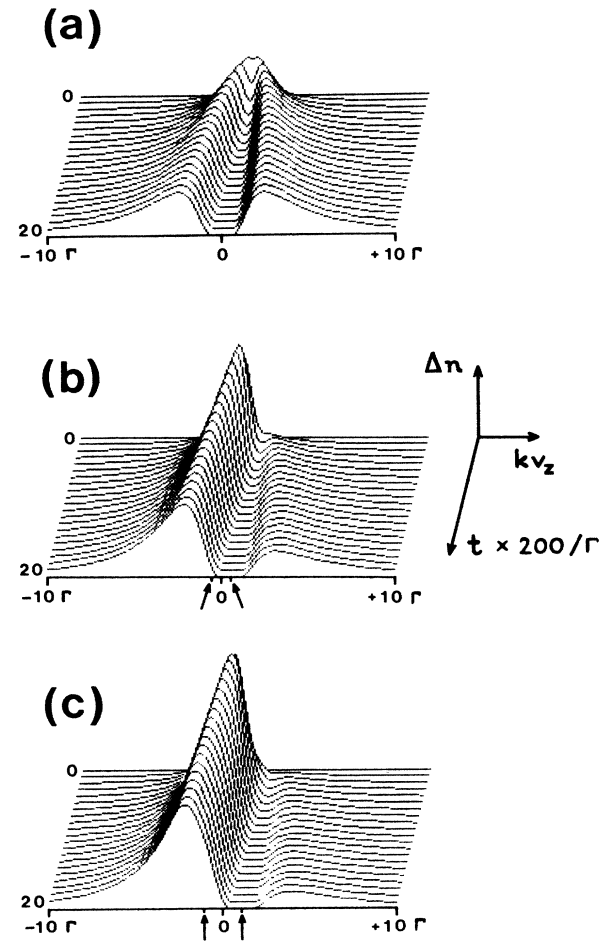

FIG. 7. $\Delta n(t,v_z)$ dependences for $\beta=\beta'=6.3\times10^{-2}\Gamma$ and various detunings (a) $\delta=0$; (b) $\delta=\frac{1}{2}\Gamma$, (c) $\delta=\Gamma$. The velocities v_z of atoms perturbed by off-resonant light beams are indicated with arrows in diagrams (b) and (c).

the transit time of an atom across the beams, which is a simple function of the transversal velocity $v_\perp$. This point will be discussed in more detail in Sec. IV C. Here we want to compare the $\langle \Delta n(t) \rangle_{v_z}$ dependence with the distribution of transit times [given by Eq. (16) below] which is plotted with a broken line in Fig. 6 for typical experimental conditions.

A full dependence of Δn on longitudinal velocities v_z, detuning δ and time t in the case of a strong probe beam ($\alpha < 1$) is shown in Fig. 7. For $\delta = 0$ [Fig. 7(a)] the probe and pump beams interact with the same longitudinal velocity class $v_z = 0$. As was already seen in Fig. 5, shortly after an atom has entered the beams at $t = 0$ polarization Δn builds up due to the pump-beam action, whereas later the depletion due to pumping by the probe beam takes place, leading to a dip in the lower-state population difference. For the off-resonance excitation ($\delta \neq 0$) both beams perturb different velocity classes and their competition (buildup and depletion of Δn) becomes more pronounced [Figs. 7(b) and 7(c)].

C. Transit-time effects

As it was already noted, standard steady-state approaches with phenomenological transit relaxation constants are not appropriate when atomic transit times across the light beams are comparable with the pumping times. Under such circumstances time-dependent solutions for $\Delta n(t)$ have to be found and averaged over various transit times or, equivalently, transversal velocities of individual atoms. For a complete velocity averaging in Eq. (12) the integration over longitudinal velocity components has to be performed. Both averagings are independent in our case and, in principle, may be performed in any order but it seems more natural to integrate firstly over $v_\perp$ (over transit times) and then over v_z.

We assume Maxwellian velocity distribution of atoms in the cell,

$$W(\mathbf{v}) = W(v_z) W(v_\perp) ,$$

with

$$W(v_z) = \frac{1}{u\sqrt{\pi}} e^{-(v_z/u)^2} , \tag{14}$$

and

$$W(v_\perp) = \frac{2v_\perp}{u^2} e^{-(v_\perp/u)^2} , \tag{15}$$

where $u = (2k_B T/M)^{1/2}$ is the most probable velocity.

Since for the geometry such as in Fig. 2 interaction time $t = R/v_\perp$, one may derive from the $W(v_\perp)$ distribution a corresponding one of the transit times,

$$W(t) = \frac{2R}{tu^2} e^{-(R/tu)^2} . \tag{16}$$

$W(t)$ is depicted in Fig. 6 with a broken line for typical experimental conditions, i.e., $R = 3$ mm, $u = 500$ m/s.

Thanks to the relation between t and $v_\perp$, and between the $W(t)$ and $W(v_\perp)$ distributions, the transit-time-averaged populations

$$N_i = \int_0^\infty n_i(t) W(t) dt ,$$

can be calculated as

$$N_i = \int_0^\infty n_i \left[\frac{R}{v_\perp} \right] W(v_\perp) dv_\perp .$$

Details of such an averaging are given in Ref. 10; here we simply write the averaged ΔN

$$\begin{aligned} \Delta N &= \int_0^\infty \Delta n(t(v_\perp)) W(v_\perp) dv_\perp \\ &= A[F(B_-) - F(B_+)] , \end{aligned} \tag{17}$$

where $A = (\mathcal{N}_0/2)(I_s/\alpha T)$, and

$$B_\pm = T(1 \pm \alpha) \frac{R}{u} , \tag{18}$$

$$F(x) = \int_0^\infty e^{-x/(y)^{1/2}} e^{-y} dy . \tag{19}$$

As seen, the transit-time-average ΔN depends essentially on the dimensionless products of the average transit time R/u and the rates $T(1 \pm \alpha)$ of the time evolution of the populations [see Eqs. (9) and (13)]. Thus, useful parameters for description of the ensemble-averaged signals are the following dimensionless saturation parameters:

$$G = 4 \frac{\beta^2}{\Gamma} \frac{R}{u} ,$$

and (20)

$$G' = 4 \frac{\beta'^2}{\Gamma} \frac{R}{u} .$$

The last step of velocity averaging in Eq. (12) is calculation of the integral

$$d\beta' \int_{-\infty}^{\infty} \frac{\Delta N}{\Omega_+} W(v_z) dv_z = \mathcal{R} + i\mathcal{I} , \tag{21}$$

where $\mathcal{R}$ and $\mathcal{I}$ are real and imaginary components, respectively, of the probe-beam electric field associated with the dispersive ($\mathcal{R}$) and absorptive ($\mathcal{I}$) properties of the medium.

Finally, we get the probe-beam signal for exactly crossed polarizers

$$\begin{aligned} I_{PS} &\sim (d\beta')^2 \left| \int_{-\infty}^{\infty} dv_z \frac{W(v_z)}{\Omega_+} \int_0^\infty \Delta n W(v_\perp) dv_\perp \right|^2 \\ &= (d\beta')^2 \left| \int_{-\infty}^{\infty} dv_z \frac{A W(v_z)}{\Omega_+} [F(B_-) - F(B_+)] \right|^2 \\ &= (d\beta')^2 (\mathcal{R}^2 + \mathcal{I}^2) . \end{aligned} \tag{22}$$

It is interesting to note that the saturation parameters in Eqs. (20) are the same as those which are used in standard steady-state approach $G = 4\beta^2/(\gamma_e \gamma_g)$ where in the low-pressure regime and with long-lived lower levels γ_g is taken as the transit rate ($\gamma_{e,g}$ being the phenomenological decay rates of the upper and lower levels, respectively). This is, however, the only similarity of our calculations with the standard approach which is incapable of repro-

ducing the line shapes given by Eq. (22), except for very weak light intensities where the first terms of power-series expansions of $F(x)$ could be used.

Because of complicated, nonanalytical integrals in Eq. (22) the theoretical probe-beam signals have to be computed numerically. In Fig. 8 several PS resonances are shown calculated for various values of G' and for constant value of $G=0.5$. For small G' the PS signal is a Doppler-free nearly Lorentzian resonance of a width close to the natural (homogeneous) linewidth Γ of the investigated transition. As the value of G' increases, the resonance line shape deviates from the Lorentzian one and broadens until, eventually, a dip in its center appears. This is a consequence of a corresponding dip in the $\Delta n(t)$ dependence which develops for appropriately large values of $I_p t$ (see Fig. 7). For not-too-high G' the dip could be significantly narrower than the homogeneous linewidth. Further increasing of G' does not increase the signal amplitude any more resulting only in a broadening of the central dip.

To complete the discussion of nonstationary VSOP we will analyze possible complications which may arise if the given atomic system has several close but distinct lines.

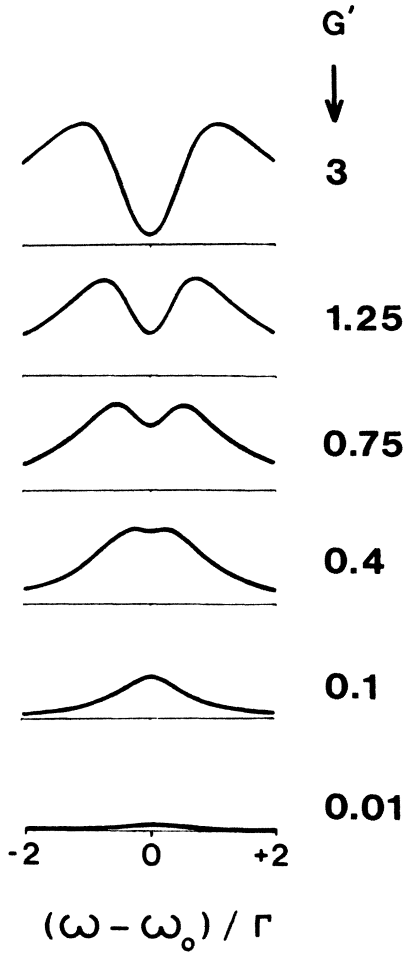

FIG. 8. Doppler-free PS resonances calculated for saturation parameters $G=0.5$ and various values of G'.

In the case of PS such complications are threefold: Firstly, the optical pumping cycles at each of the transitions could be mutually dependent; secondly, additional crossover resonances may appear because of coupled transitions; thirdly, new interference contributions would appear in the net signal. The first two complications occur when the lines are coupled either by a common level or by spontaneous emission and, in general, require solving equations much more complicated than in the above model. The third complication, on the other hand, is universal in a way in that it occurs for coupled as well as for uncoupled transitions. In the latter case simple analysis of the interference effects could be performed with the help of the model developed in this paper.

If there are n uncoupled distinct transitions which contribute to the net PS signal then the resulting electric field of the probe beam is

$$E=\sum_{i=1}^{n}(\mathscr{R}_i+i\mathscr{I}_i)+\mathscr{B}+i\mathscr{U} ,$$

where $\mathscr{B}+i\mathscr{U}$ is a constant coherent background, which could be introduced by, e.g., uncrossed polarizers or a phase retarder between them, and $\mathscr{R}_i+i\mathscr{I}_i$ are the contributions of each ith line given by Eq. (22).

The net PS signal is then

$$I_{\mathrm{PS}}\sim\sum_i\mathscr{R}_i^2+\sum_i\mathscr{I}_i^2+\mathscr{B}^2+\mathscr{U}^2+2\sum_{\substack{i,j\\(i>j)}}\mathscr{R}_i\mathscr{R}_j +2\sum_{\substack{i,j\\(i>j)}}\mathscr{I}_i\mathscr{I}_j+\mathscr{B}\sum_i\mathscr{R}_i+\mathscr{U}\sum_i\mathscr{I}_i . \quad (23)$$

The first four terms in Eq. (23) are symmetrical around each resonance frequency ω_0^i, while the last ones which arise from the mutual interference between contributions due to various transitions and from the interference between the background and atomic contributions are asymmetrical. As in the standard Doppler-free PS,[3,4] in the considered case where the transit-time effects are important the mutual interference also may severely distort the resulting line shapes. In some cases, however, this distortion may be compensated by a proper choice of the coherent background. Another paper[18] brings a detailed discussion of an influence of the interference effects on the PS signals with subnatural dips in the case of two close uncoupled lines.

V. CONCLUSIONS

The time-dependent analysis of nonstationary (transit) effects of velocity-selective optical pumping effects has been performed with a simple four-level model. It is limited to weak light intensities but as is well known[1-8] the VSOP phenomena occur just for weak excitation. As in Ref. 10, no phenomenological relaxation constants are introduced to account for finite relaxation times, and the transit-time effects have been obtained as a consequence of averaging the time evolution of individual atoms moving in the light fields.

Under appropriate conditions, i.e., existence of a trap level, suitable interaction times, and strong probe beam,

nonstationary velocity-selective optical pumping with two counterpropagating laser beams (tuned to one-photon transition) may lead to very strong modification (formation of the dip) in the population distribution of the long-lived lower-state sublevels with respect to the steady-state distribution. Such a modification is in turn responsible for the appearance of the narrow dip in the center of a homogeneously broadened Doppler-free signal in polarization spectroscopy. Our results are therefore complementary to those by Bjorkholm *et al.*[10] who have been probing an excited-state population in two-photon spectroscopy.

It is noteworthy that the dips in PS signals could be significantly narrower than the natural linewidth Γ, and that they occur in the vapor phase. Most experiments where subnatural resolution was obtained have been performed with collimated atomic beams to get rid of the large Doppler width. Our results illustrate that the use of the beams is not essential if another Doppler-free technique, appropriate for a gas phase, is employed.

The appearance of the dip is the most spectacular consequence of nonstationarity of VSOP. As in the case described in Ref. 10, its origin has not been immediately realized. The interpretation based on the first observations[11] with sodium has been refuted by more refined later measurements.[12] Details of those measurements and a discussion of the properties and possible spectroscopic applications of such subnatural dips based on the results of this work are published elsewhere.[18] Here we wish only to point out that the subnatural dips do not allow the resolution of the lines frequency separation of which is less than Γ. Still, we wish to emphasize the possibility of using the dips to study, e.g., subtle shifts of isolated lines in a low-pressure vapor phase with a high resolution or for laser frequency stabilization.

ACKNOWLEDGMENTS

This work was supported by the Polish Research Program under Contract No. MRI-5 (CPBP 1.06). The author would like to express his thanks to Professor G. zu Putlitz and all the colleagues from the Physikalisches Institut der Universität Heidelberg for very warm hospitality he had experienced during his stay in Heidelberg. Thanks are also due to Dr. J. Zachorowski for valuable comments on the manuscript.

APPENDIX: DERIVATION OF THE RATE EQUATIONS

We start with the density-matrix equation

$$\dot{\rho}=-\frac{i}{\hbar}[\mathscr{H},\rho]\ , \tag{A1}$$

where $\mathscr{H}=\mathscr{H}_0-\mathbf{E}\cdot\mathbf{D}$, and $\mathscr{H}_0$ contains the terms responsible for spontaneous emission from level $|0\rangle$ (Fig. 1). If the strong-field standing-wave effects are not taken into account and if the rotating-wave approximation is made, the elements of ρ which are responsible for optical coherences could be written as

$$\begin{aligned}\rho_{0+}&=i\beta'_+r_+e^{-i(\omega t+kz)}\ ,\\ \rho_{0-}&=i\beta R_-e^{-i(\omega t-kz)}-i\beta'_-R_+e^{-i(\omega t+kz)}\ ,\end{aligned} \tag{A2}$$

where the Rabi frequencies $\beta,\beta'_\pm$ are defined in Eq. (3), R_+ and r_+ are slowly varying envelopes of the contributions to the optical coherences due to the probe beam, and R_- is the envelope of the contribution due to the pump beam.

In the following we will assume weak intensities of the light beams and neglect Zeeman coherence ρ_{+-}. Also any possible nonradiative relaxation is neglected, the only incoherent parts in the Hamiltonian $\mathscr{H}$ being related with spontaneous emission from the $|0\rangle$ state to the lower states $|+\rangle$, $|-\rangle$, and $|1\rangle$.

Under such conditions the following set of equations for envelopes r_+, $R_\pm$, and populations n_i is obtained from (A1):

$$\begin{aligned}\dot{r}_+&=i\Omega_+r_++n_+-n_0\ ,\\ \dot{R}_+&=i\Omega_+R_++n_--n_0\ ,\\ \dot{R}_-&=i\Omega_-R_-+n_--n_0\ ,\\ \dot{n}_0&=-\beta'^2_+(r_++r^*_+)\\ &\quad-\beta'^2_-(R_++R^*_+)-\beta^2(R_-+R^*_-)-\Gamma n_0\ ,\end{aligned} \tag{A3}$$

$$\begin{aligned}\dot{n}_+&=\beta'^2_+(r_++r^*_+)+p_+\Gamma n_0\ ,\\ \dot{n}_-&=\beta'^2_-(R_++R^*_+)+\beta^2(R_-+R^*_-)+p_-\Gamma n_0\ ,\\ \dot{n}_1&=p_1\Gamma n_0\ ,\end{aligned} \tag{A4}$$

where $\Omega_\pm=\delta\pm kv_z-i\Gamma/2$.

For $\beta,\beta'_\pm\ll\Gamma$, and $t\gg\Gamma^{-1}$ evolution of populations is much slower than $e^{-\Gamma t}$ and integration of Eqs. (A3) results in

$$\begin{aligned}r_+(t)&=[n_0(t)-n_+(t)]/(i\Omega_+)\ ,\\ R_+(t)&=[n_0(t)-n_-(t)]/(i\Omega_+)\ ,\\ R_-(t)&=[n_0(t)-n_-(t)]/(i\Omega_-)\ ,\end{aligned}$$

which substituted into Eqs. (A4) yield readily the rate equations (4) of Sec. III.

[1]M. Pinard, C. G. Aminoff, and F. Laloë, Phys. Rev. A **19**, 2366 (1979).

[2]D. E. Murnick, M. S. Feld, M. M. Burns, T. U. Kühl, and P. G. Pappas, in *Laser Spectroscopy IV,* edited by H. Walther and K. W. Rothe (Springer, Berlin, 1979), p. 195; Opt. Lett. **5**, 79 (1980).

[3]W. Gawlik and G. W. Series, in *Laser Spectroscopy IV,* edited by H. Walther and K. W. Rothe (Springer, Berlin, 1979), p. 210.

[4]S. Nakayama, G. W. Series, and W. Gawlik, Opt. Commun.

34, 382 (1980).

[5]P. G. Pappas, M. M. Burns, D. D. Hinshelwood, M. S. Feld, and D. E. Murnick, Phys. Rev. A **21**, 1955 (1980).

[6]H. Rinneberg, T. Huhle, E. Matthias, and A. Timmerman, Z. Phys. A **295**, 17 (1980).

[7]S. Nakayama, J. Phys. Soc. Jpn. **50**, 606 (1981).

[8]W. Gawlik, Acta Phys. Pol. A **66**, 401 (1984).

[9]J. E. Thomas and W. W. Quivers Jr., Phys. Rev. A **22**, 2115 (1980).

[10]J. E. Bjorkholm, P. F. Liao, and A. Wokaun, Phys. Rev. A **26**, 2643 (1982).

[11]W. Gawlik, J. Kowalski, F. Träger, and M. Vollmer, Phys. Rev. Lett. **48**, 871 (1982).

[12]W. Gawlik, J. Kowalski, F. Träger, and M. Vollmer, in *Laser Spectroscopy VI,* edited by H. P. Weber and W. Lüthy (Springer, Berlin, 1983), p. 136.

[13]J. E. Thomas and R. A. Forber, Opt. Lett. **9**, 56 (1984).

[14]C. M. Klimcak and J. C. Camparo, Phys. Rev. A **30**, 1791 (1984).

[15]S. G. Rautian and A. M. Shalagin, Pis'ma Zh. Eksp. Teor. Fiz. **9**, 686 (1969) [JETP Lett. **9**, 427 (1969)]; Zh. Eksp. Teor. Fiz. **58**, 962 (1970) [Sov. Phys.—JETP **31**, 518 (1970)]; E. V. Baklanov, B. Ya. Dubetskii, V. M. Semibalamut, and E. A. Titov, Kvant. Elektron. **2**, 2518 (1975) [Sov. J. Quant. Electron. **5**, 1374 (1976)]; S. N. Bagaev, L. S. Vasilenko, A. K. Dmitriev, M. N. Skvortsov, and V. P. Chebotaev, Pis'ma Zh. Eksp. Teor. Fiz. **23**, 399 (1976) [JETP Lett. **23**, 360 (1976)]; C. J. Bordé, J. L. Hall, C. V. Kunasz, and D. G. Hummer, Phys. Rev. A **14**, 236 (1976).

[16]F. Biraben, M. Bassini, and B. Cagnac, J. Phys. (Paris) **40**, 445 (1979).

[17]E.g., M. D. Levenson, in *Introduction to Nonlinear Laser Spectroscopy* (Academic, New York, 1982).

[18]W. Gawlik, J. Kowalski, F. Träger, and M. Vollmer, J. Phys. B (to be published).